Dynamic Experiment of a 5-Span Railway PC Bridge

Kitami Institute of Technology　Member　Yasunori Miyamori
Northeast Dianli University of China　Student Member　○Youqi Zhang
Kitami Institute of Technology　Member　Takanori Kadota
National Institute of Technology Warangal of India　Soumya Ranjan Harichandan

1. Introduction

Many bridges are built in the high economic growth period of Japan, and the maintenance method for these aging bridges are demanded. Therefore, a new structural health monitoring technique such as Smart Sensors [1,2] has attracted people's attention.

Nowadays, most of the SHM researches were focused on the element level [3,4]. Element SHM tests effectively revealed how dynamic parameters shifted after damaged, but whether the results can be applied to a complex real structure has a lot of uncertainty. So real bridge dynamic tests such as [2,5,6,7] are still required.

One main purpose of SHM is to find invisible damage of structures. However, invisible damage detecting and localization is a very challenging topic. So the objective of this research is to investigate the dynamical parameters of such multiple-span PC bridge as the fundamental study of damage detecting and localization.

2. Information of the bridge

Mukagawa Bridge is a 5-span pre-stressed concrete railway bridge which construction was completed in 1977. The bridge lies over Muka River (Mukagawa) in Kitami City. Bridge length is 158.8m, and span length is about 31.3m. The service of the bridge has been stopped for several years. Sleepers and tracks were destructed before tests. A general view of the bridge was shown in Fig.1 and the different heights of abutments and piers were shown in Fig. 2.

3. Dynamic tests on Mukagawa Bridge

3.1. Layout of the experiment

The dynamic characteristics of Mukagawa Bridge were identified by 2 sets of vibration tests. Both Set 1 and Set 2 had 5 tests. In total 10 tests were carried out. Sensor distribution maps and detail locations were shown in Fig. 3.

Set 1 (Test 1~5) aimed to identify the dynamic characteristics of every single span. 10 Imote2 with SHM-H Smart Sensors were installed uniformly in both side of one span. Excitation method was 2 people jumping and landing on the deck synchronously in the middle of the span.

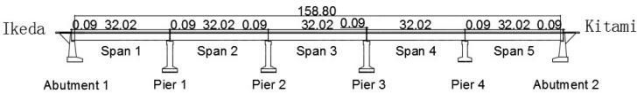

Fig. 1　General view of Mukagawa Bridge

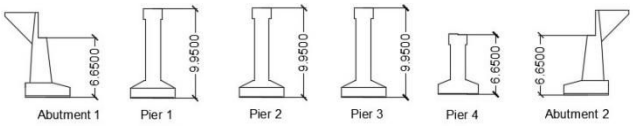

Fig. 2　Length of abutments and piers

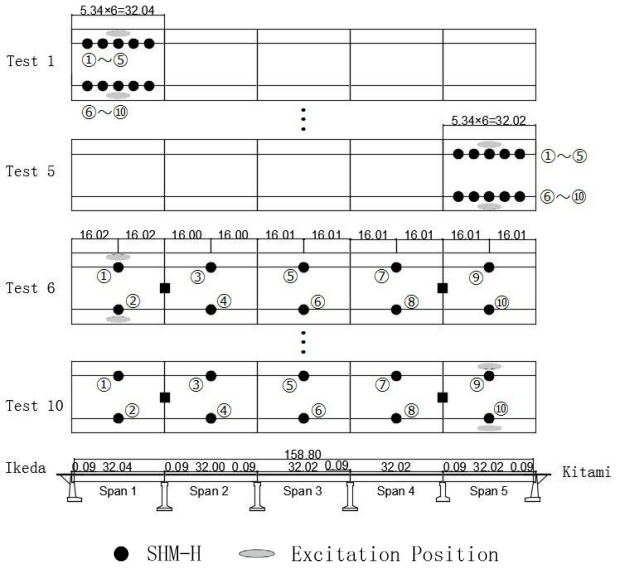

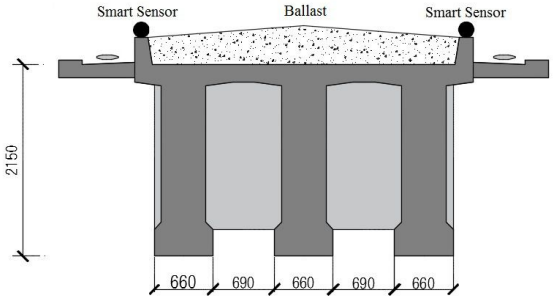

Fig. 3　Smart Sensor distribution map

Set 2 (Test 6~10) aimed to identify the dynamic characteristics of the whole bridge. There were 9cm gaps between adjacent spans. But ballast which were used to fix and support sleepers and tracks before were continuously and uniformly distributed on the deck from Span 1 to Span 5. If the

stiffness of ballast and interaction between ballast and girders were taken into consideration, all spans were connected into one frame structure by ballast. So in Set 2, dynamic tests of the whole bridge were carried out. 10 SHM-H Smart Sensors and 2 Imote nodes were used simultaneously. 2 SHM-H Smart Sensors were installed in the middle point of each span. 2 Imote nodes were fixed on tripods and only used to transmit wireless signal. Excitation method was 2 people jumping and landing on the deck synchronously in the middle of the assigned span.

3.2. Data processing method

In every test, 10 channels of z direction data was collected from 10 Imote2 with SHM-H Smart Sensors. All collected acceleration data was analyzed by Fourier transforming, after that frequency domain power spectrum was obtained. Predominant frequencies were identified by peak picking method and damping was calculated by half-power method. Finally, experimental modal shapes were calculated by cross spectrum method.

4. Modal analysis results

4.1 Set 1 tests analysis result

Natural frequencies and modes of Span 1~5 were identified from Set 1 (Test 1~5) tests. Natural frequencies of Span 1~5 were shown in Table.1 and four modal shapes were shown in Table.2. The identified natural frequencies and modal shapes of Span 1~5 were summarized as follows. The 1st and 4th modes were bending modes. The 2nd and 3rd modes were torsional modes.

The 1st and 2nd modal frequencies of Span 2 and Span 3 were significantly lower than Span 1, Span 4 and Span 5. In this case, the difference of span length during construction was not the main reason to cause this phenomenon. The height difference of 2 abutments and 4 piers should be firstly considered to understand this appearance. Girders in Span 1~5 were same designed with same section and reinforcement, and all girders had same type of line bearing supports. However, Pier 4 was evidently shorter than other piers. When the structure vibrated, the displacement on supports were very small. So if girders in one span and the abutment or piers were considered as one rigid frame structure as Fig.4, this phenomenon could be easily explained. If the length of girder was a constant value, the longer the piers were, the lower natural frequency the girder-piers frame structure had.

There was no obvious difference between the 3rd modal frequencies of every span. So we can get the conclusion that the higher torsional modal frequency of girders were not sensitive to the height of piers.

The 4th modal frequencies of every span were not as concentrated as the 3rd modal frequencies. But Span 2 and Span 3 which connected with higher piers also had relatively low 4th modal frequencies. Span 5 was supported by the lowest pier and abutment, so Span 5 had the highest frequency. Span 1 had the lowest 4th modal frequency, this abnormal phenomenon might give some hint about damage detection, so in future researches, Span 1 should be given priority to inspect.

Table. 1　Natural frequencies (Hz) of Span 1~5

Span	Mode 1		Mode 2	
	Frequency	Damping	Frequency	Damping
1	4.2046	0.0073	7.623	0.0112
2	3.9311	0.0124	7.1786	0.0088
3	3.9995	0.0095	6.8368	0.0101
4	4.3414	0.0062	8.4092	0.0067
5	4.1074	0.0071	8.4092	0.0073
Span	Mode 3		Mode 4	
	Frequency	Damping	Frequency	Damping
1	21.3307	0.0076	27.6547	0.0222
2	21.2965	0.0064	28.3726	0.0168
3	21.3307	00099	28.0649	0.0126
4	21.9802	0.0057	29.9451	0.0055
5	21.9802	0.0051	30.1843	0.0093

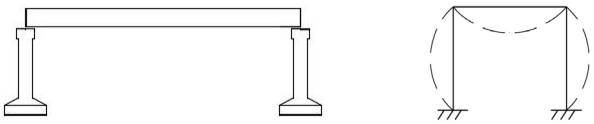

Fig. 4. Girder-piers rigid frame structure

4.2 Set 2 tests analysis result

Power spectrum of Test 7 was showed in Fig.5, and frequency axis was assigned from 3Hz to 5Hz to show the detail interaction of lower bending modal frequency of every span. According to the result of Set 1 tests in Table 1~2, lower bending modal frequency of every span was different, and Span 2 had the lowest lower bending modal frequency. However, in Fig.5, Span 2 Span 3 and Span 5 had same lower bending modal frequencies as the results of Set 1 tests. There was a pronounced peak at 3.9311Hz (lower bending frequency of Span 2) on all spans. But Span 3~5 also had another peak. Span 3 and Span 5 kept their own lower bending frequency, but Span 4 decreased its lower bending frequency. Overview from the power spectrum from Span 1 to Span 5, for the excitation span, there would be one obvious peak of lower bending modal frequency, and for other no excitation spans, the peak of the lower bending modal frequency of Span 2 can be maintained as the crossing red line in Fig.5, at the same time, the lower bending modal frequencies of their own could also be kept.

Fig.6 was the general view of power spectrum of Test 6, and the frequency axis was assigned from 3Hz to 10Hz.The predominant modal shape of every channel of Set 2 tests were summarized in Table.3. Table.3 and Fig.6 showed that in these tests, the excitation spans' bending modal frequencies had

Table. 2　First four modes of Span 5 dynamic testing

Span	Mode 1	Mode 2	Mode 3	Mode 4
1	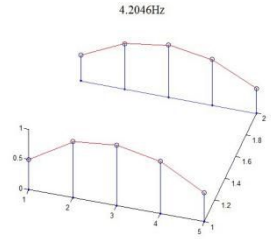	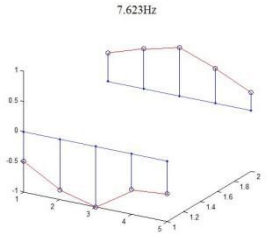	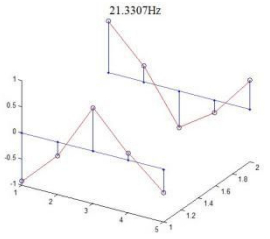	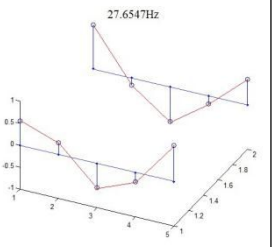
2	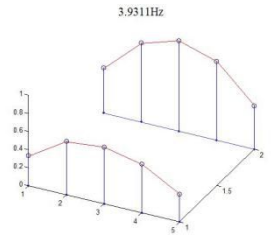	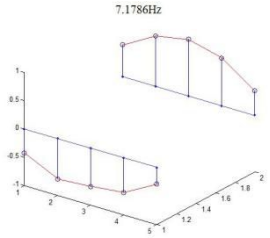	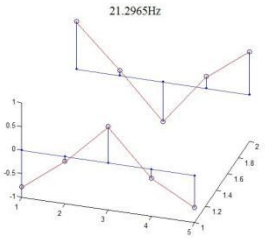	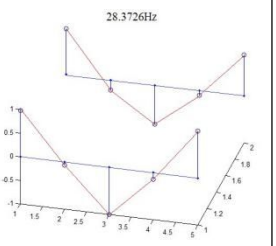
3	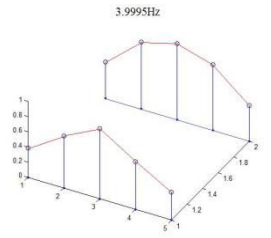	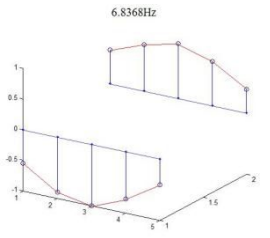	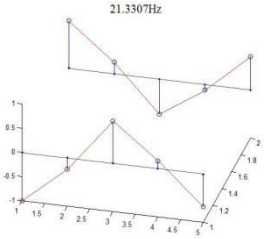	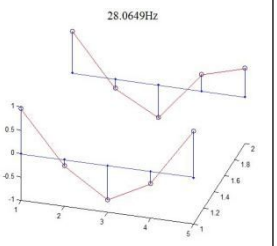
4	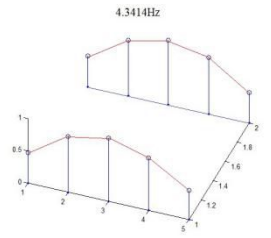	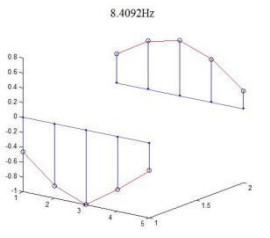	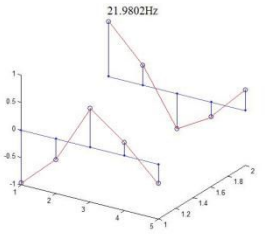	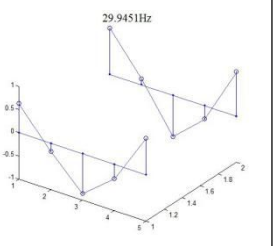
5	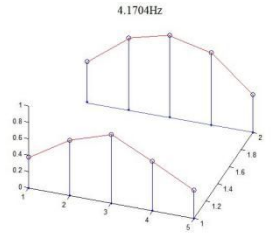	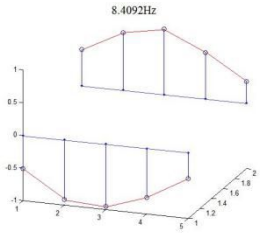	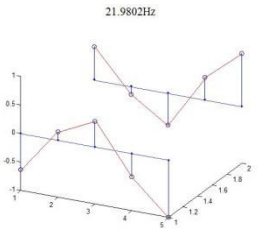	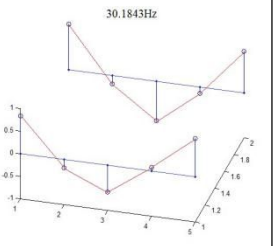

the highest magnitude than other no excitation spans, and in these excitation spans predominant mode was lower bending mode. On adjacent spans of excitation spans, the predominant mode could be both lower bending mode and lower torsional mode. But the lower torsional mode had a higher probability to become to the predominant mode. For furthest spans, lower torsional mode was the predominant mode. Overview of Table 3, one phenomenon could be found that there was a trend that from excitation spans to the furthest spans predominant mode would change from lower bending mode to lower torsional mode. The reason to cause these phenomena should be that high frequency vibration could transmit more easily than low frequency vibration in ballast.

5. Conclusions

In this paper, an application of dynamic testing for the characterization of a 5-span PC bridge has been presented.

The first part of the analysis was devoted to the accurate extraction of modal parameters from frequency response function measurements of every single span. Some important indications emerged from the experiment. Firstly, in a real 5-span PC bridge, the calculation of vibration modal frequency

of every single span should consider the heights of piers or abutment to get a higher accuracy. The girder should combine with the abutment or piers beside into a girder-piers frame structure. Secondly, lower bending and lower torsional modal frequencies are sensitive to this effect, higher bending and higher torsional modal frequencies are not sensitive to this effect.

The second part of the work was addressed to discuss the dynamic response and interaction of all spans. Conclusion can be summarized as 2 points. For the first point, the interaction between excitation span and no excitation spans manifested as the lower bending modal frequency peak of excitation span could be maintained by other spans, and no excitation spans would kept their own lower bending modal frequency peaks. For the second point, farther spans from the excitation span were more likely to behave the lower torsional modes as the predominant modes.

This research is the fundamental study of structural health monitoring. And it is the first step to detect the invisible damage of structure. Further tests are still demand to have a better understanding of this not ideal multiple-span continuous simply-supported girder bridge in reality.

6. Acknowledgements

This research was supported by JSPS Grant-in-Aid for Scientific Research(C) Grant Number 15K06176. The contribution of Mr. Itsuki Nakashima, Mr. Shuuta Todori, Dr. Tomoyuki Yamazaki and Mr. Yutaka Tsubota was greatly acknowledged.

7. Reference

1) T. Nagayama, Jr. B. F. Spencer, Structural Health Monitoring using Smart Sensors, NSEL Report Series, No.1, University of Illinois at Urbana-Champaign (2007).
2) T. Kadota, Y. Miyamori, R. Watasaki, S. Mikami, T. Saito, Structural vibration characteristics of a pedestrian bridge by the 3D acceleration sensing of smart sensors and detailed 3D-FEM modal, IABSE Symposium Report 104 (2015), 1-8.
3) C. Sbarufatti, G. Manson, K. Worden, A numerically-enhanced machine learning approach to damage diagnosis using a Lamb wave sensing network, Journal of Sound and Vibration. 333(2014), 4499–4525.
4) G. Tondreau, A. Deraemaeker, Automated data-based damage localization under ambient vibration using local modal filters and dynamic strain measurements: Experimental applications, Journal of Sound and Vibration, 333(2014), 7364–7385 .
5) D. Siringoringo, Y. Fujino, and T. Nagayama, Dynamic Characteristics of an Overpass Bridge in a Full-Scale Destructive Test. Journal of Engineering Mechanics, Vol. 139, No. 6, (2013), 691-701.
6) T. Türker, A. Bayraktar, Structural safety assessment of bowstring type RC arch bridges using ambient vibration testing and finite element modal calibration, Measurement, Volume 58, (2014), 33-45.
7) M. Dilena, A. Morassi, Dynamic testing of a damaged bridge, Mechanical Systems and Signal Processing, 25, (2011), 1485–1507.

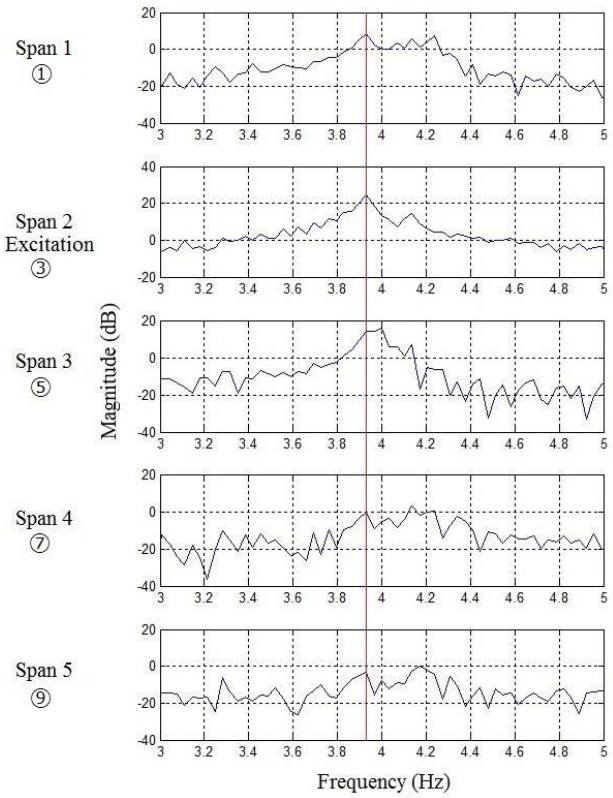

Fig. 5　Power Spectrum of Chanel 1, 3, 5, 7, 9 of Test 7

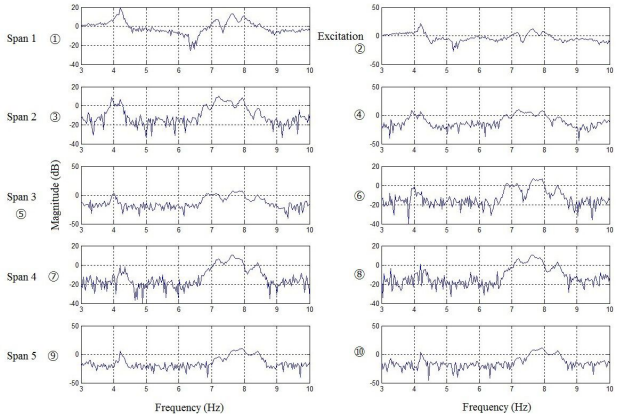

Fig. 6　Power Spectrum of Test 6

Table. 3　Predominant mode of all channels in Test 6~10

	Span 1	Span 2	Span 3	Span 4	Span 5
Test 6	B	T	T	T	T
	B	T	T	T	T
Test 7	T	B	T	T	T
	T	B	T	T	T
Test 8	T	T	B	T	T
	T	B	B	T	T
Test 9	T	B	B	B	B
	T	B	B	B	B
Test 10	T	T	T	T	B
	T	T	T	T	B

Annotation: B: Bending mode was the predominant mode; T: Torsional mode was the predominant mode; Forms in shadow: The span was the excitation location.